forming one class are the planetary waves, in which the time evolution is prompted by the weak but important *planetary effect*.

As we may recall from Section 2-6, on a spherical earth (or planet or star, in general), the Coriolis parameter, f, is proportional to the rotation rate, Ω, times the sine of the latitude, φ:

$$f = 2\Omega \sin \varphi .$$

Large wave formations such as alternating cyclones and anticyclones contributing to our daily weather and, to a lesser extent, the Gulf Stream meanders span several degrees of latitude; for them, it is necessary to consider the meridional change in the Coriolis parameter. If the coordinate y is oriented northward and is measured from a reference latitude φ_0 (say, a latitude somewhere in the middle of the wave under consideration), then $\varphi = \varphi_0 + y/a$, where a is the earth's radius (6371 km). Considering y/a as a small departure, the Coriolis parameter can be expanded in a Taylor series:

$$f = 2\Omega \sin \varphi_0 + 2\Omega \frac{y}{a} \cos \varphi_0 + \cdots \tag{6-15}$$

Retaining only the first two terms, we write in traditional notation

$$f = f_0 + \beta_0 y, \tag{6-16}$$

where $f_0 = 2\Omega \sin \varphi_0$ is the reference Coriolis parameter and $\beta_0 = 2(\Omega/a) \cos \varphi_0$ is the *beta parameter*. Typical midlatitude values on Earth are $f_0 = 8 \times 10^{-5} \cdot s^{-1}$ and $\beta_0 = 2 \times 10^{-11}\ m^{-1} \cdot s^{-1}$. The Cartesian framework where the beta term is not retained is called the *f-plane*, and that where it is retained is called the *beta plane*. The next step in order of accuracy is to retain the full spherical geometry (which we will avoid throughout this book). Rigorous justifications of the beta-plane approximation can be found in Veronis (1963, 1981), Pedlosky (1987), and Verkley (1990).

Note that the beta-plane representation is validated at mid latitudes only if the $\beta_0 y$ term is small compared to the leading f_0 term. In terms of the motion's meridional length scale L, this implies

$$\beta = \frac{\beta_0 L}{f_0} \ll 1, \tag{6-17}$$

where the dimensionless ratio can be called the *planetary number*.

The governing equations, having become

$$\frac{\partial u}{\partial t} - (f_0 + \beta_0 y) v = -g \frac{\partial \eta}{\partial x}, \tag{6-18a}$$

$$\frac{\partial v}{\partial t} + (f_0 + \beta_0 y) u = -g \frac{\partial \eta}{\partial y}, \tag{6-18b}$$

$$\frac{\partial \eta}{\partial t} + H \left(\frac{\partial u}{\partial x} + \frac{\partial v}{\partial y} \right) = 0, \tag{6-18c}$$

are now mixtures of small and large terms. The larger ones (f_0, g, and H terms) comprise the otherwise steady, f-plane geostrophic dynamics; the smaller ones (time derivatives and β_0 terms) come as perturbations, which, although small, will govern the wave evolution. In first approximation, the large terms dominate, and thus $u \simeq -(g/f_0)\partial\eta/\partial y$ and $v \simeq (g/f_0)\partial\eta/\partial x$. Use of this first approximation in the small terms of (6-18a) and (6-18b) yields

$$-\frac{g}{f_0}\frac{\partial^2\eta}{\partial y\partial t} - f_0 v - \frac{\beta_0 g}{f_0}\, y\, \frac{\partial\eta}{\partial x} = -g\frac{\partial\eta}{\partial x} \tag{6-19a}$$

$$+\frac{g}{f_0}\frac{\partial^2\eta}{\partial x\partial t} + f_0 u - \frac{\beta_0 g}{f_0}\, y\, \frac{\partial\eta}{\partial y} = -g\frac{\partial\eta}{\partial y}. \tag{6-19b}$$

These equations are trivial to solve with respect to u and v:

$$u = -\frac{g}{f_0}\frac{\partial\eta}{\partial y} - \frac{g}{f_0^2}\frac{\partial^2\eta}{\partial x\partial t} + \frac{\beta_0 g}{f_0^2}\, y\, \frac{\partial\eta}{\partial y} \tag{6-20a}$$

$$v = +\frac{g}{f_0}\frac{\partial\eta}{\partial x} - \frac{g}{f_0^2}\frac{\partial^2\eta}{\partial y\partial t} - \frac{\beta_0 g}{f_0^2}\, y\, \frac{\partial\eta}{\partial x}. \tag{6-20b}$$

These last expressions can be interpreted as consisting of the leading and first-correction terms in a regular perturbation series of the velocity field. We identify the first term of each expansion as the geostrophic velocity. By contrast, the next and small terms are called *ageostrophic*.

Final substitution in continuity equation (6-18c) leads to a single equation for the surface displacement:

$$\frac{\partial\eta}{\partial t} - R^2\frac{\partial}{\partial t}\nabla^2\eta - \beta_0 R^2\frac{\partial\eta}{\partial x} = 0, \tag{6-21}$$

where ∇^2 is the two-dimensional Laplace operator and $R = \sqrt{gH}/f_0$ is the deformation radius, defined in (6-10) and now suitably amended to be a constant. Unlike the original set of equations, this last equation has constant coefficients and a solution of the Fourier type, $\cos(lx + my - \omega t)$, can be sought. The dispersion relation follows:

$$\omega = -\beta_0 R^2 \frac{l}{1 + R^2\,(l^2 + m^2)}, \tag{6-22}$$

providing the frequency ω as a function of the wave-number components l and m. The waves are called *planetary waves* or *Rossby waves*, in honor of Carl-Gustaf Rossby, who first proposed this wave theory to explain the movement of midlatitude weather patterns. We note immediately that if the beta corrections had not been retained ($\beta_0 = 0$), the frequency would have been nil. This is the $\omega = 0$ solution of Section 6-3, which corresponds to a steady geostrophic flow on the f-plane. The absence of the other two roots is explained by our approximation. Indeed, treating the time derivatives as small terms (i.e., having in effect assumed a very small temporal Rossby number, $Ro_T \ll 1$), we have retained only the low frequency, the one much less than f_0.

That the frequency given by (6-22) is indeed small can be verified easily. With L ($\sim 1/l \sim 1/m$) as a measure of the wavelength, two cases can arise: either $L \lesssim R$ or $L \gtrsim R$; the frequency scale is then given, respectively, by

$$\text{Shorter waves:} \quad L \lesssim R, \qquad \omega \sim \beta_0 L \tag{6-23}$$

$$\text{Longer waves:} \quad L \gtrsim R, \qquad \omega \sim \frac{\beta_0 R^2}{L} \lesssim \beta_0 L . \tag{6-24}$$

In either case, our premise in (6-17) that $\beta_0 L$ is much less than f_0 implies that ω is much smaller than f_0 (subinertial wave), as we anticipated.

Let us now explore other properties of planetary waves. First and foremost, the zonal phase speed

$$c_x = \frac{\omega}{l} = \frac{-\beta_0 R^2}{1 + R^2 (l^2 + m^2)} \tag{6-25}$$

is always negative, implying a phase propagation to the west (Figure 6-4). The sign of the meridional phase speed $c_y = \omega/m$ is undetermined, since the wave number m may

Wind-driven ocean circulations (cont)

Equatorial current and counter-currents

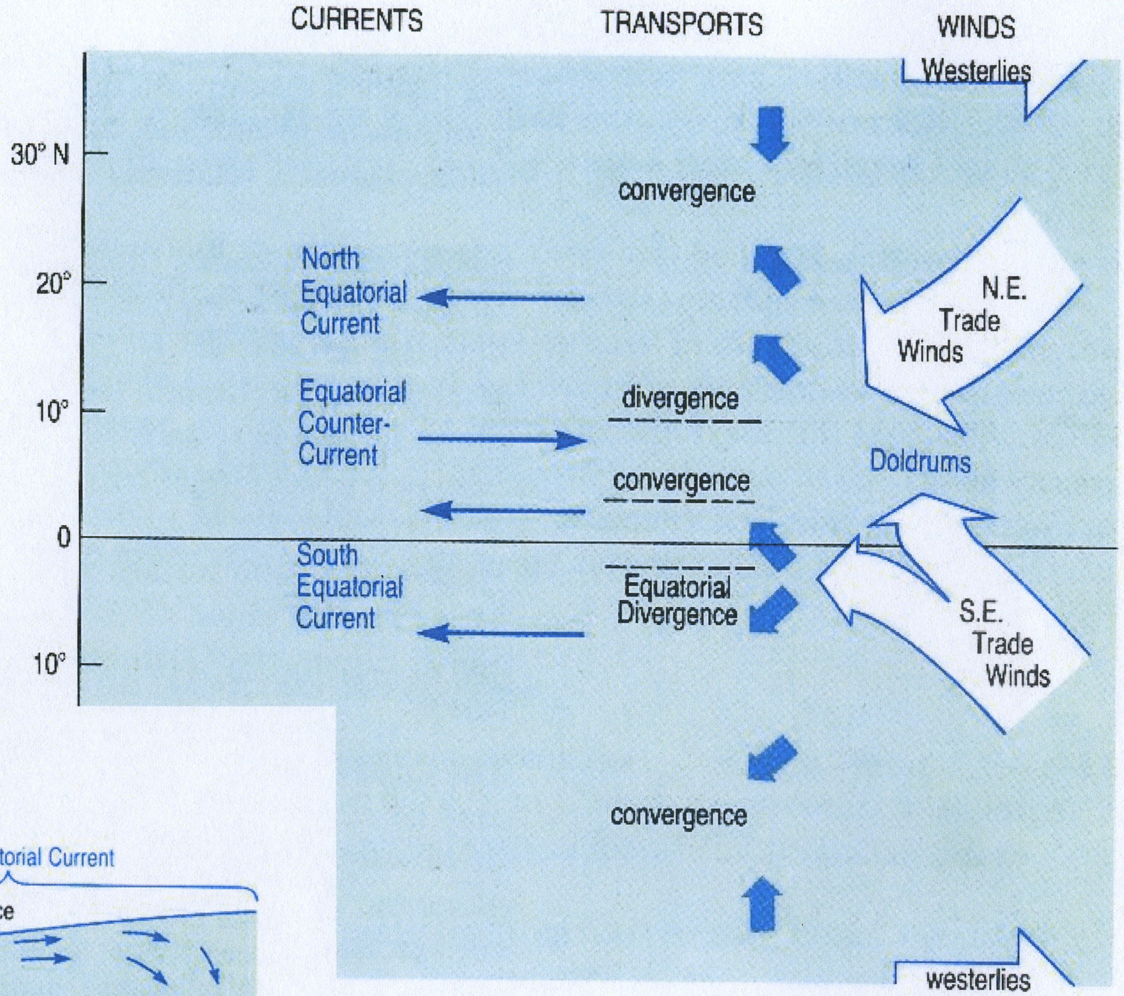

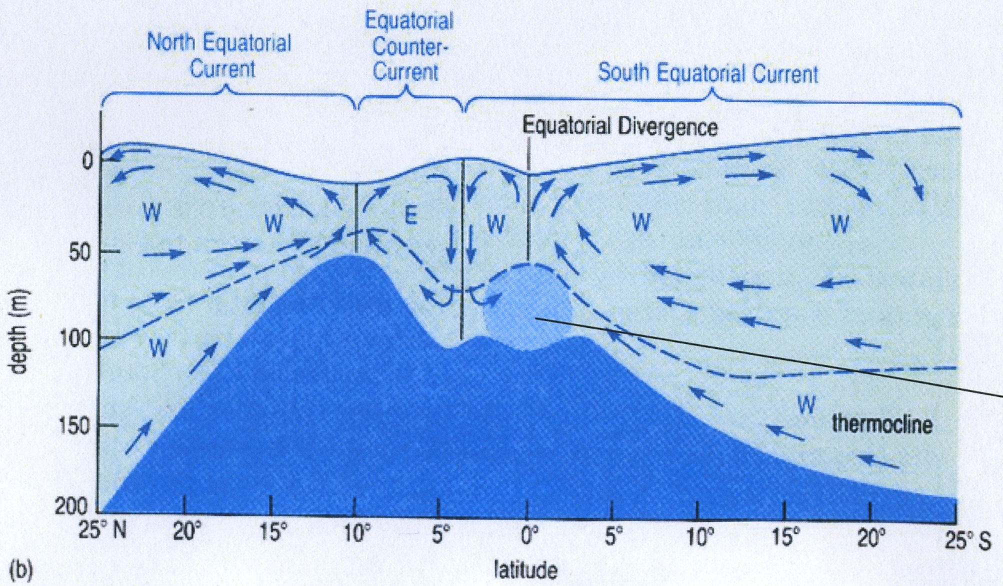

Equatorial undercurrent

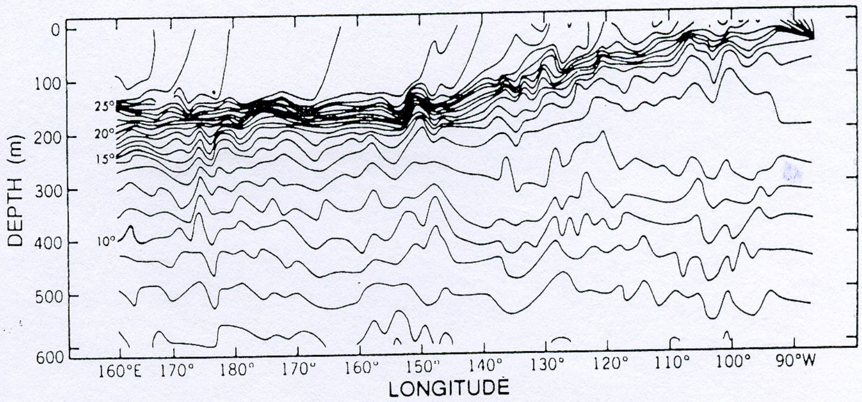

Figure 19-1 Temperature (°C) as a function of depth and longitude along the equator in the Pacific Ocean as measured in 1963 by Colin et al. (1971). Note the strong thermocline between 100 m and 200 m.

$$\frac{\partial u}{\partial t} - \beta_0 y v = -g' \frac{\partial \eta}{\partial x}, \tag{19-5a}$$

$$\frac{\partial v}{\partial t} + \beta_0 y u = -g' \frac{\partial \eta}{\partial y}, \tag{19-5b}$$

$$\frac{\partial \eta}{\partial t} + H\left(\frac{\partial u}{\partial x} + \frac{\partial v}{\partial y}\right) = 0. \tag{19-5c}$$

Here u and v are, respectively, the zonal and meridional velocity components, g' is the reduced gravity $g\Delta\rho/\rho_0$ ($= 0.02$ m/s^2), and η is the layer-thickness variation (measured positively downward).

The preceding set of equations admits a solution with zero meridional flow. With $v = 0$, (19-5a) through (19-5c) then reduce to

$$\frac{\partial u}{\partial t} = -g' \frac{\partial \eta}{\partial x}, \qquad \frac{\partial \eta}{\partial t} + H \frac{\partial u}{\partial x} = 0,$$

having any function of $x \pm ct$ and y as its solution. The remaining equation, (19-5b), sets the meridional structure, which for a signal decaying away from the equator is given by

$$u = cF(x - ct)\ e^{-y^2/2R_{eq}^2}, \tag{19-6a}$$

$$v = 0, \tag{19-6b}$$

$$\eta = HF(x - ct)\ e^{-y^2/2R_{eq}^2}, \tag{19-6c}$$

where $F(\ )$ is an arbitrary function of its argument and $R_{eq} = (c/\beta_0)^{1/2}$ is the equatorial radius of deformation introduced in the preceding section. This solution describes a

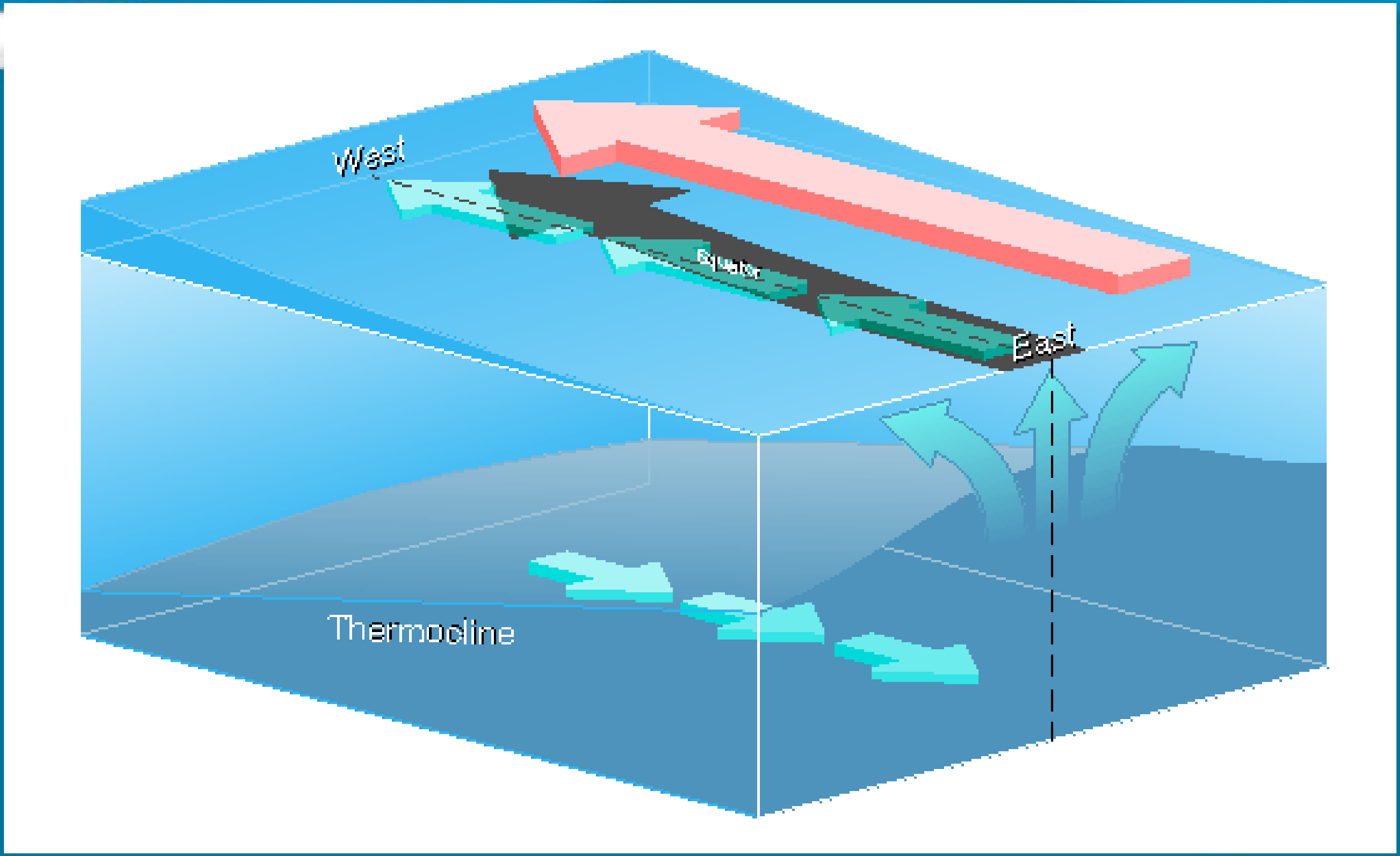
West
Equator
East
Thermocline

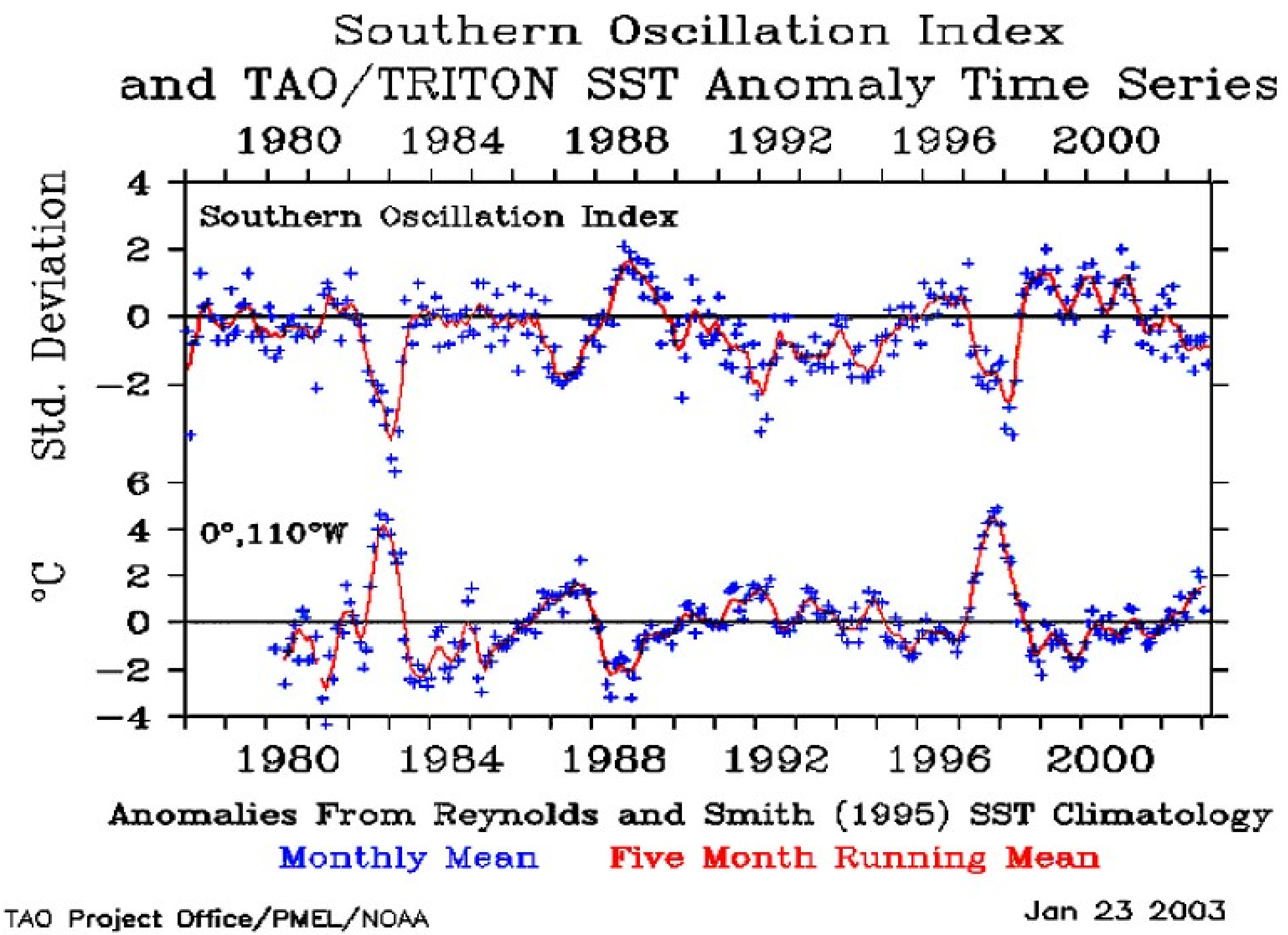

Fig. 2. Time series of the Southern Oscillation Index (SOI) (top panel) and eastern equatorial SST's (lower panel). Negative SOI values indicate El Niño conditions; positive values are associated with La Niña.

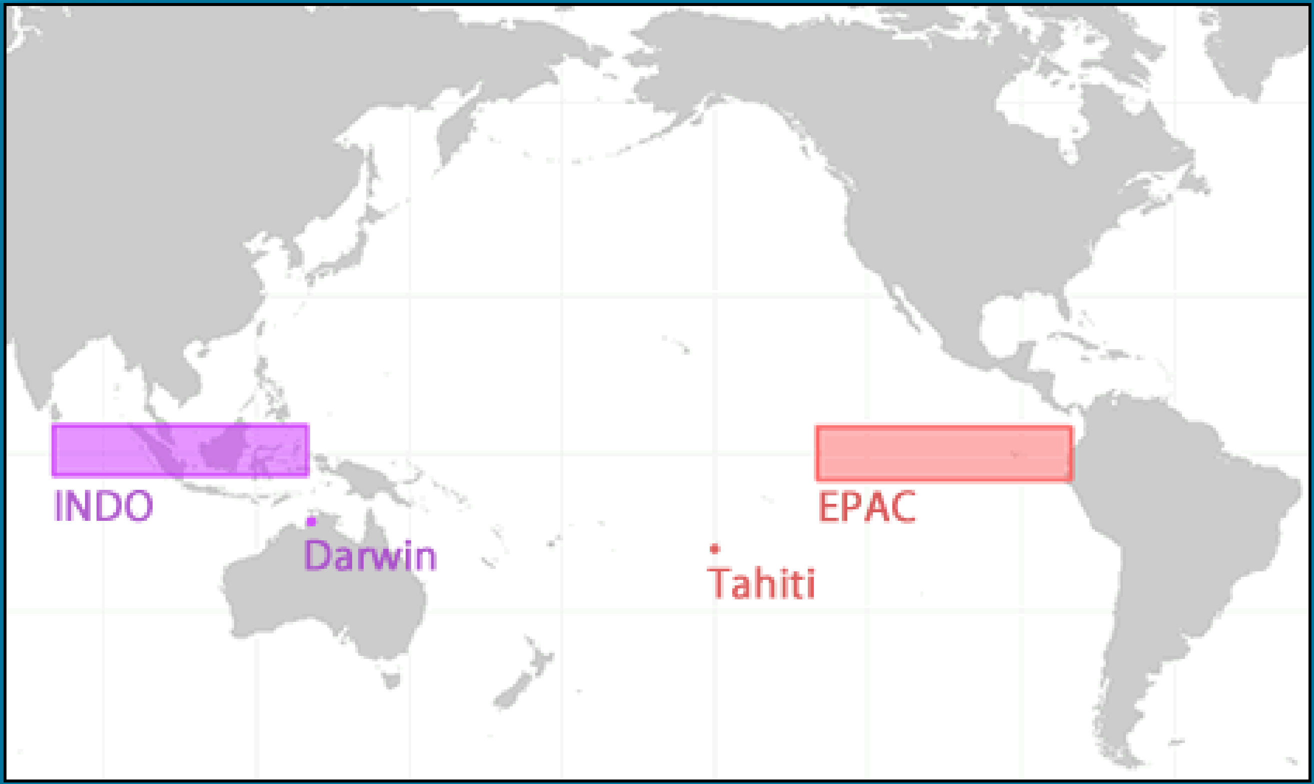
INDO
Darwin
Tahiti
EPAC

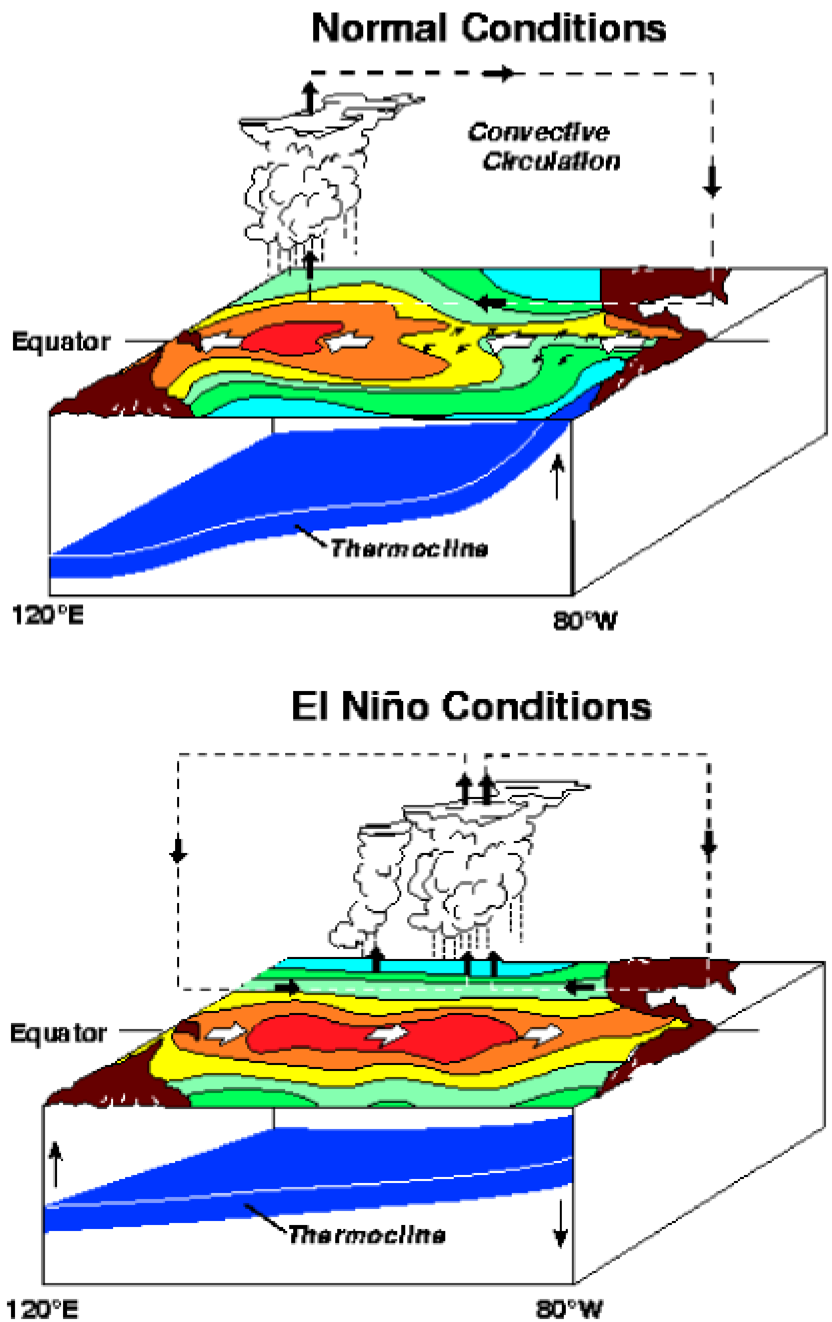
Normal Conditions
Convective Circulation
Equator
Thermocline
120°E
80°W
El Niño Conditions
Equator
Thermocline
120°E
80°W

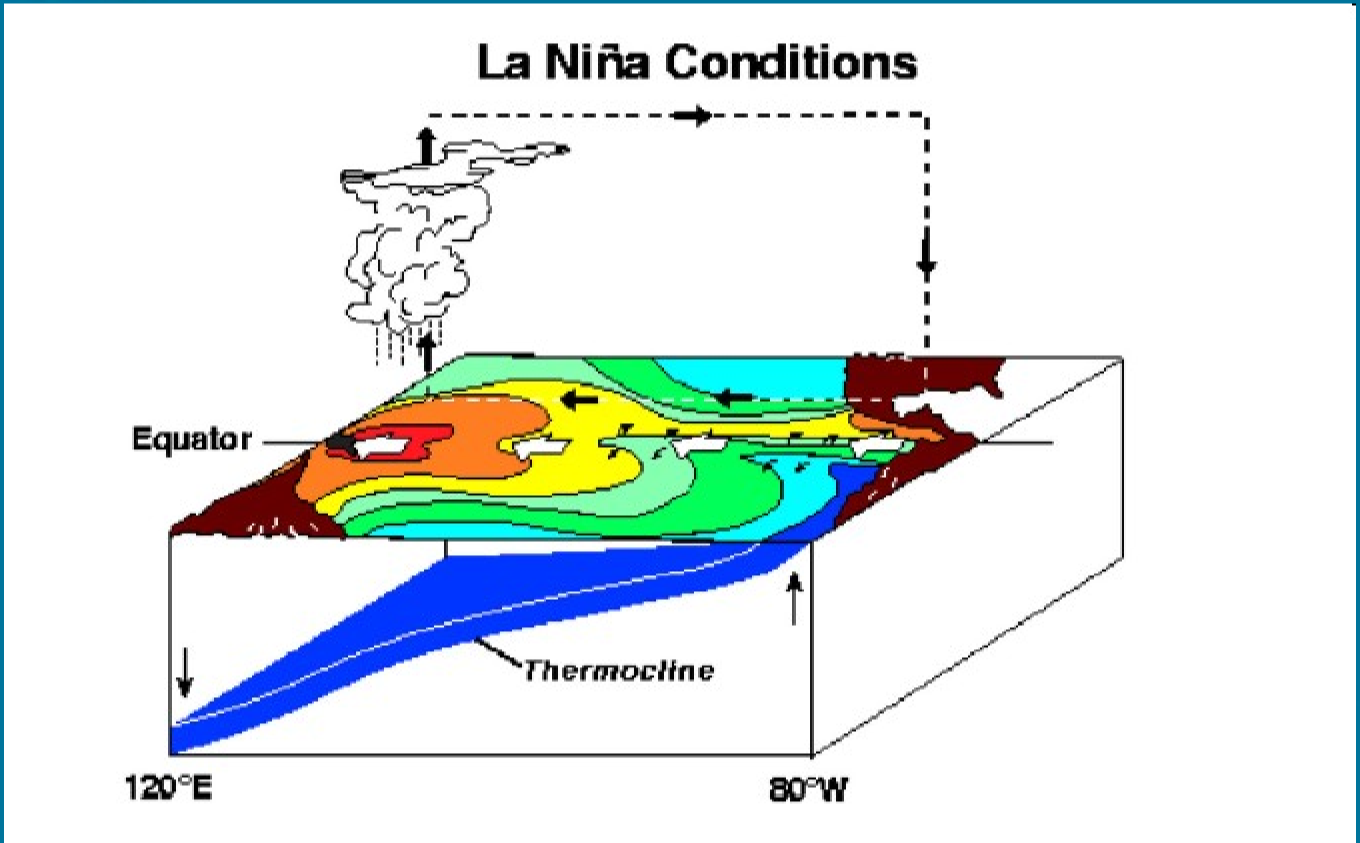
La Niña Conditions
Equator
Thermocline
120°E
80°W

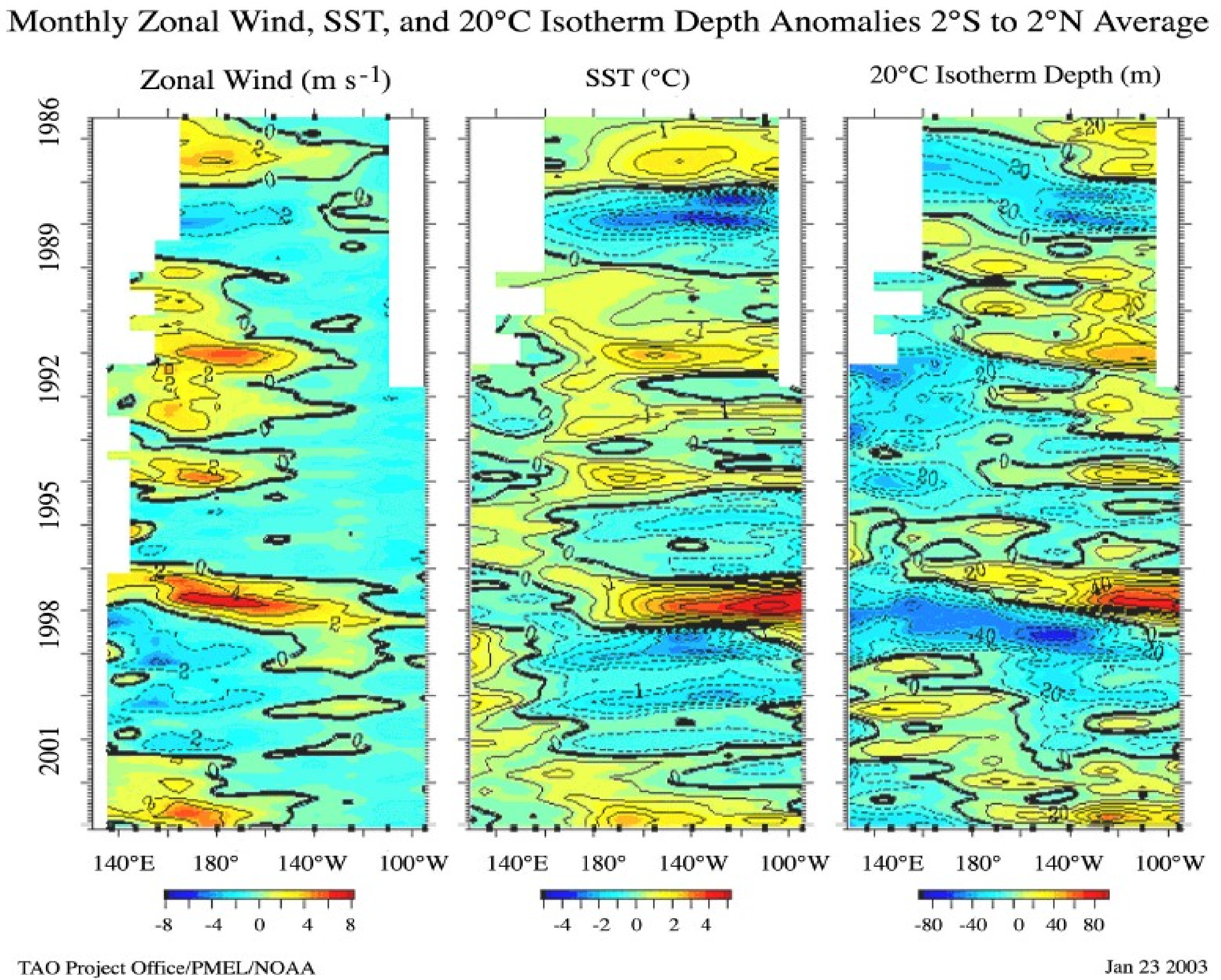

Fig. 3. Longitude-time plots along the Equator of a) zonal wind anomalies, b) SST anomalies and c) thermocline depth anomalies.

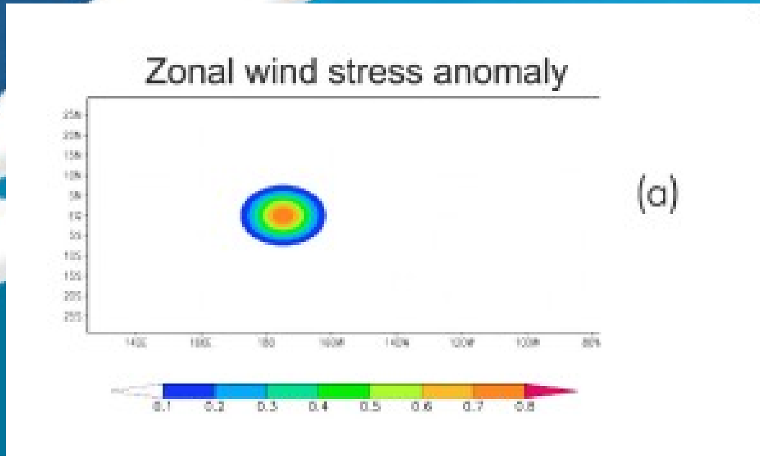
Zonal wind stress anomaly
(a)
0.1
0.2
0.3
0.4
0.5
0.6
0.7
0.8

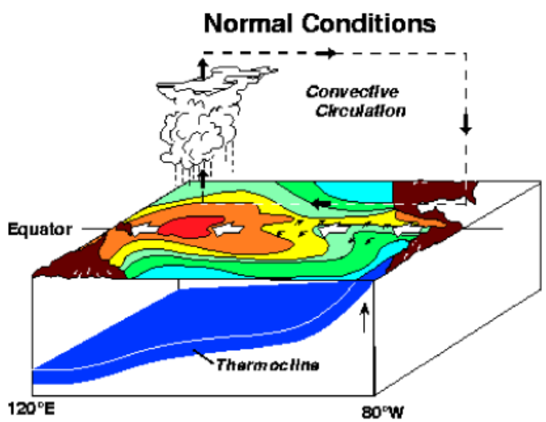
Normal Conditions
Convective Circulation
Equator
Thermocline
120°E
80°W

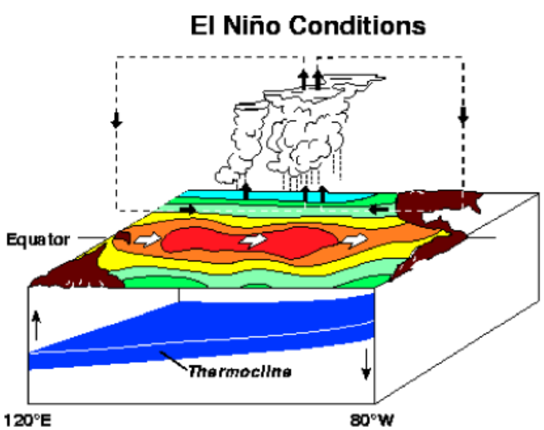
El Niño Conditions
Equator
Thermocline
120°E
80°W

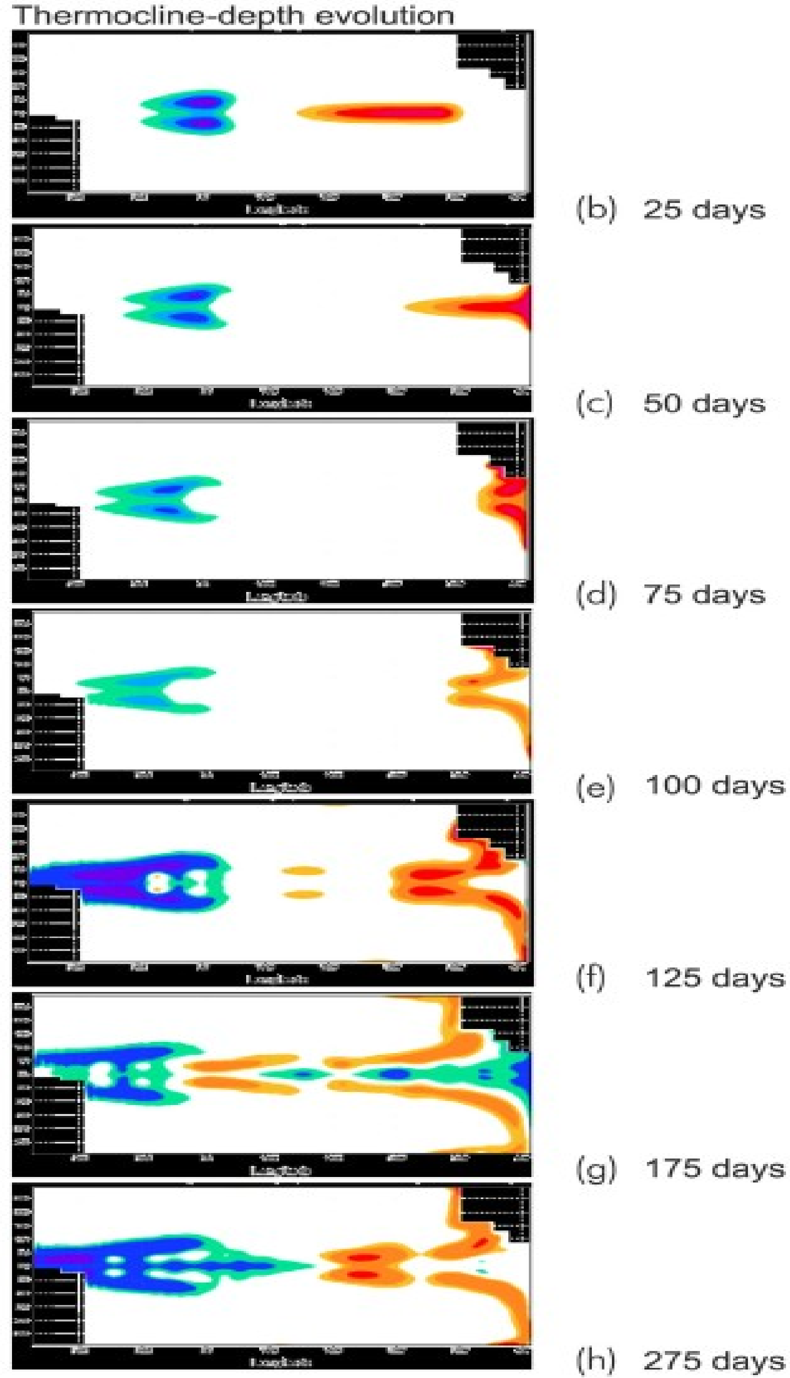
Thermocline-depth evolution
(b) 25 days
(c) 50 days
(d) 75 days
(e) 100 days
(f) 125 days
(g) 175 days
(h) 275 days

El Niño Weather Patterns December - February

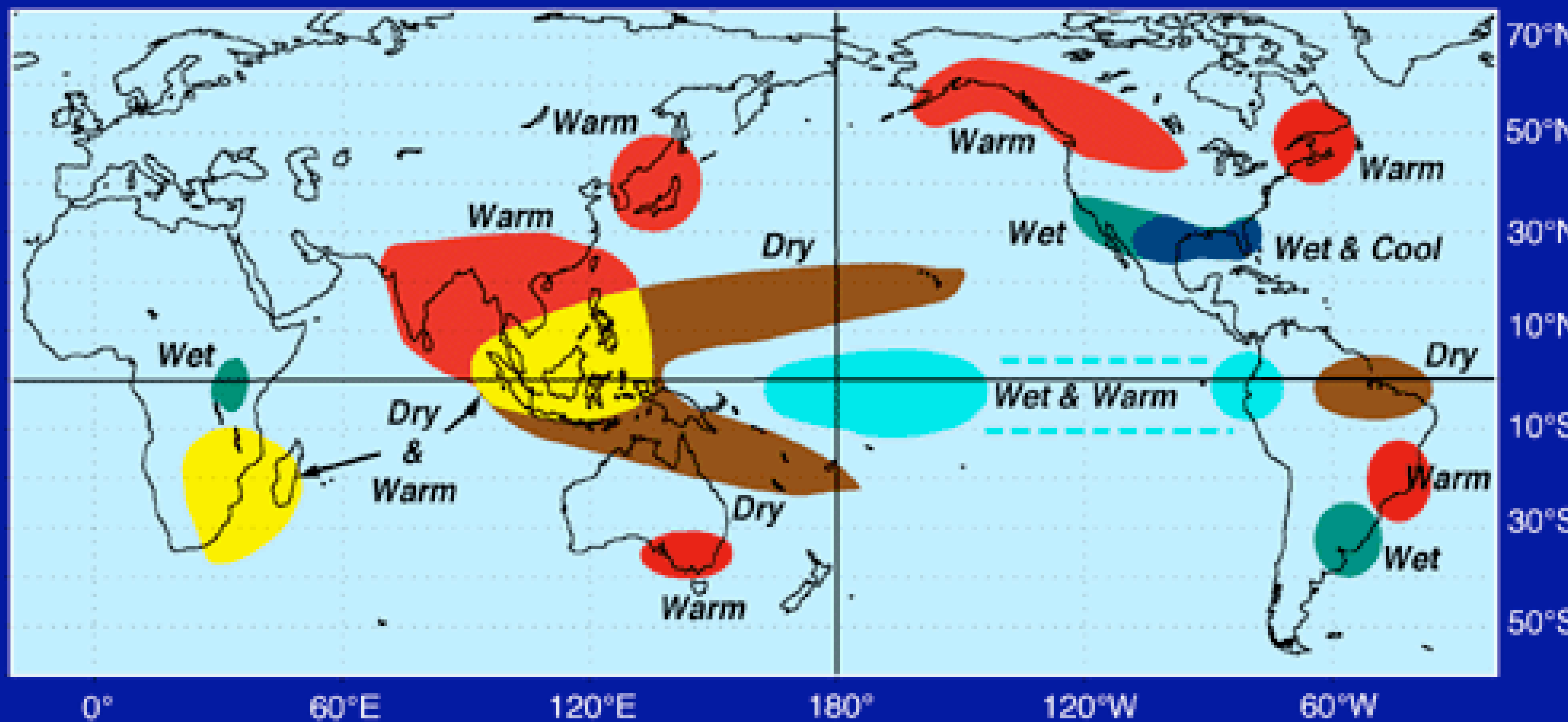

El Niño Weather Patterns June - August

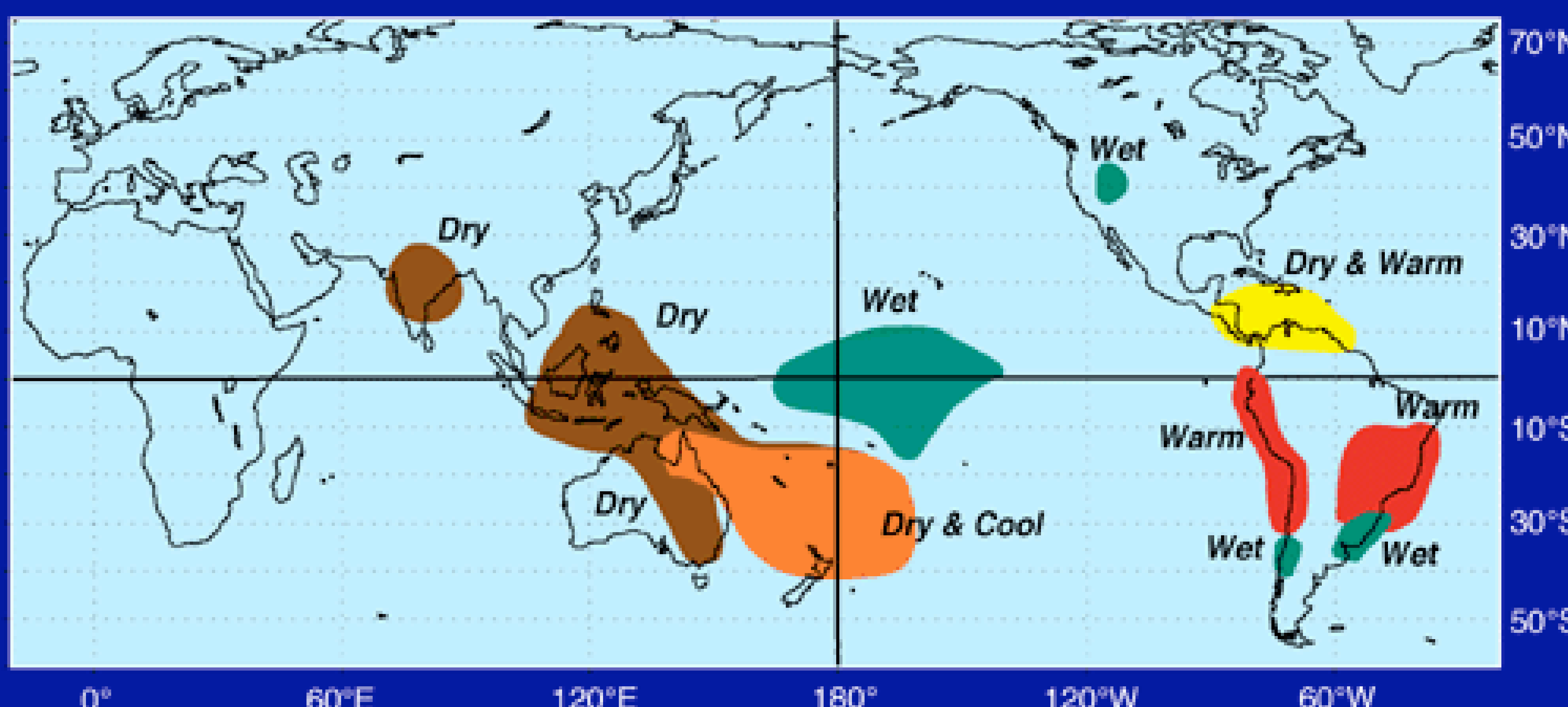

ENSO Forecasting

There are two steps in forecasting the effects of El Niño:

1. Predicting SST anomalies in the tropical Pacific
2. Using those SSTs to predict the effects on distant weather

Step 1 is based on having high-quality data coverage of the tropical Pacific to initialize models of the ocean-atmosphere system. To a large extent these models rely on projecting waves into the future. Such forecasts can be made for 6-9 months.

Step 2 uses ordinary weather forecast models, initialized with the predicted tropical SSTs.

Since weather is highly chaotic, a large ensemble of model runs must be made to understand the results.

An example of ensemble forecasting

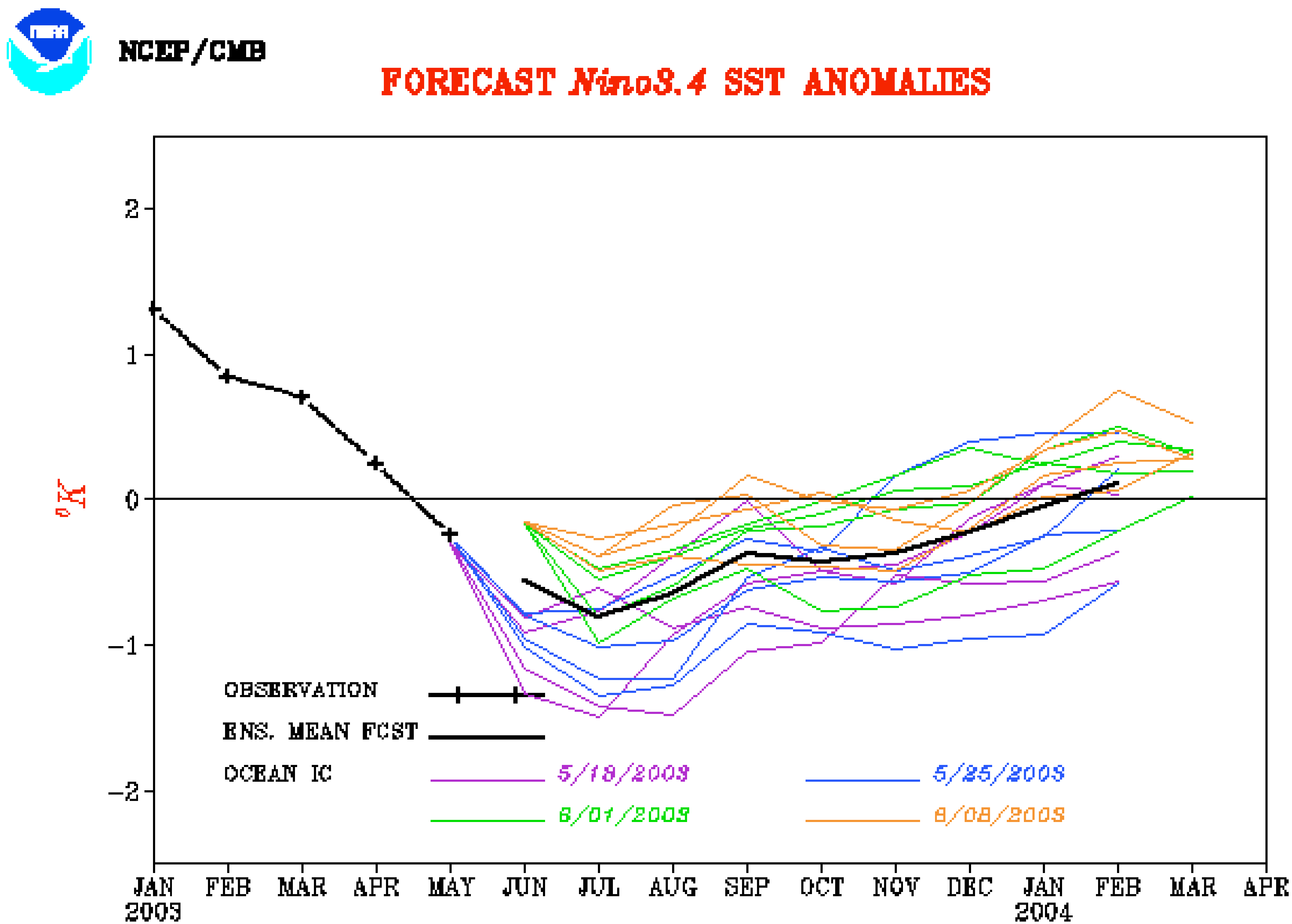

Last Update: Tue Jun 24 2003

How well did the forecasts do?

NCEP/CMB

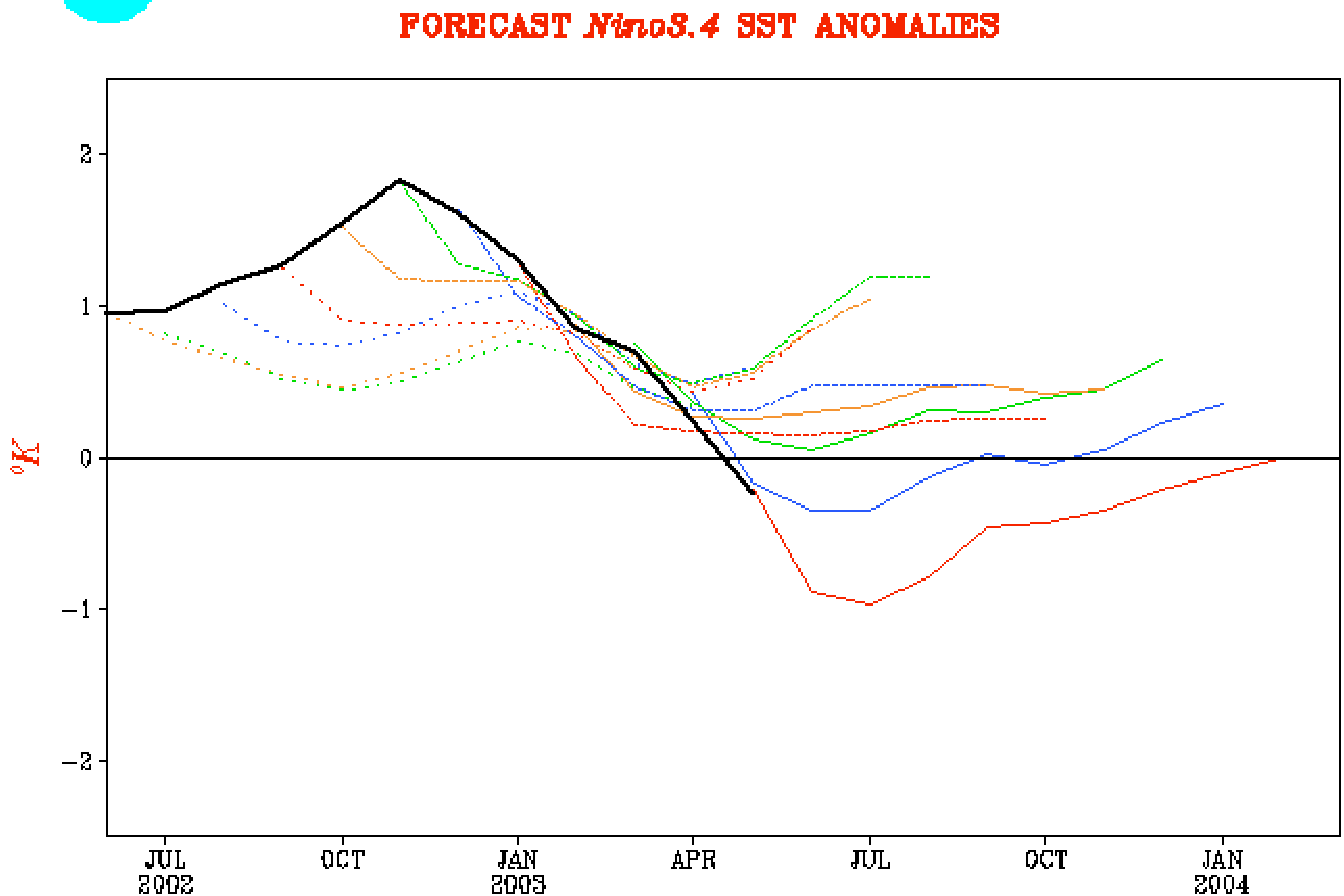

Forecasts are drawn in colors and observation is drawn in black.

Last Update: Tue Jun 10 2003

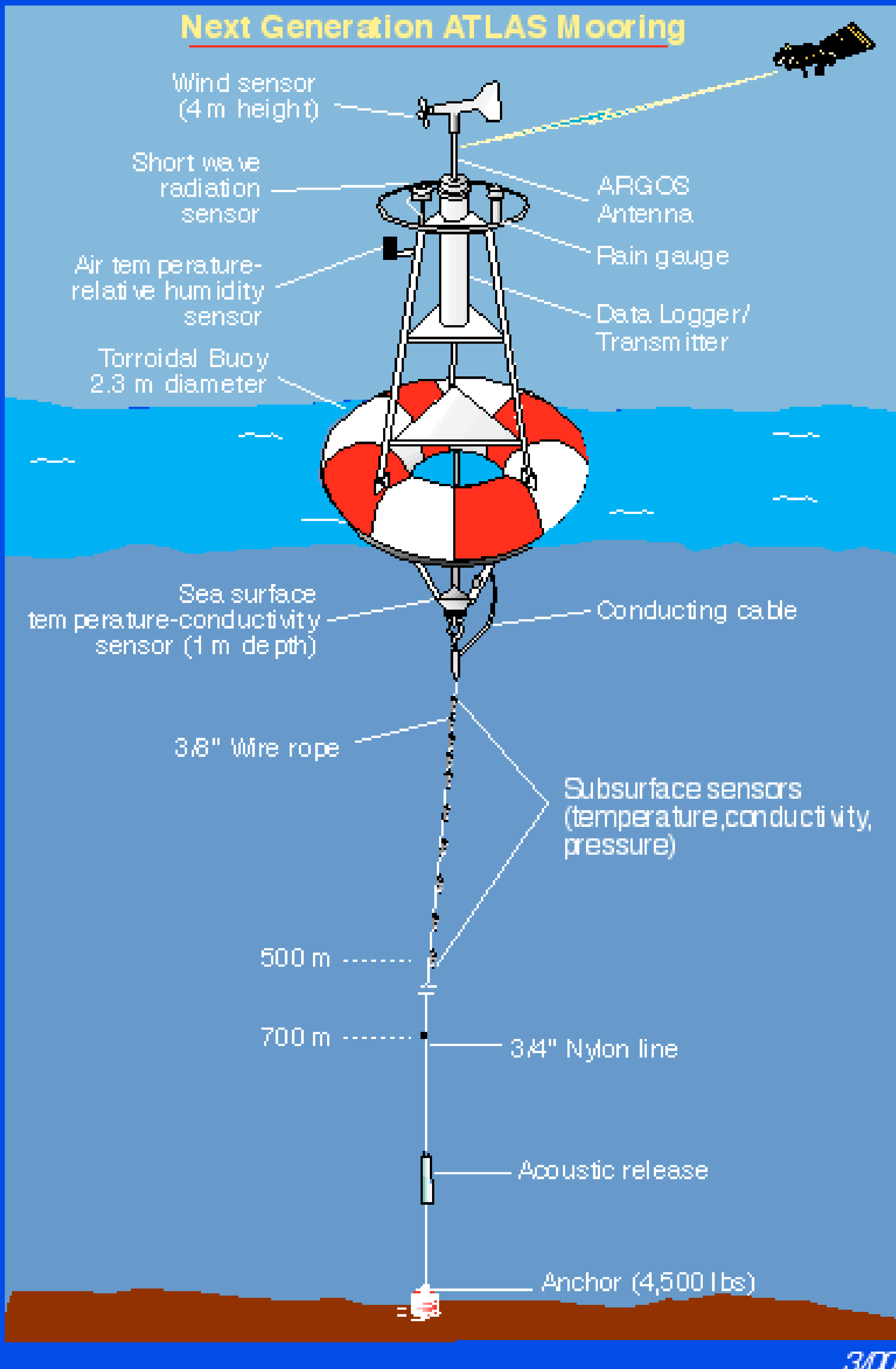

A TAO mooring

A principal mission of this laboratory is to provide the data sufficient to describe the state of the tropical Pacific for input into the forecast models.

The ATLAS mooring was developed at PMEL in the 1980s and is our primary tool. The moorings last for a year or more (and the parts are reusable), and all data are received in near-real time.


ATLAS

The TAO-TRITON network is a US-Japan project. There are 70 moorings maintained continuously.

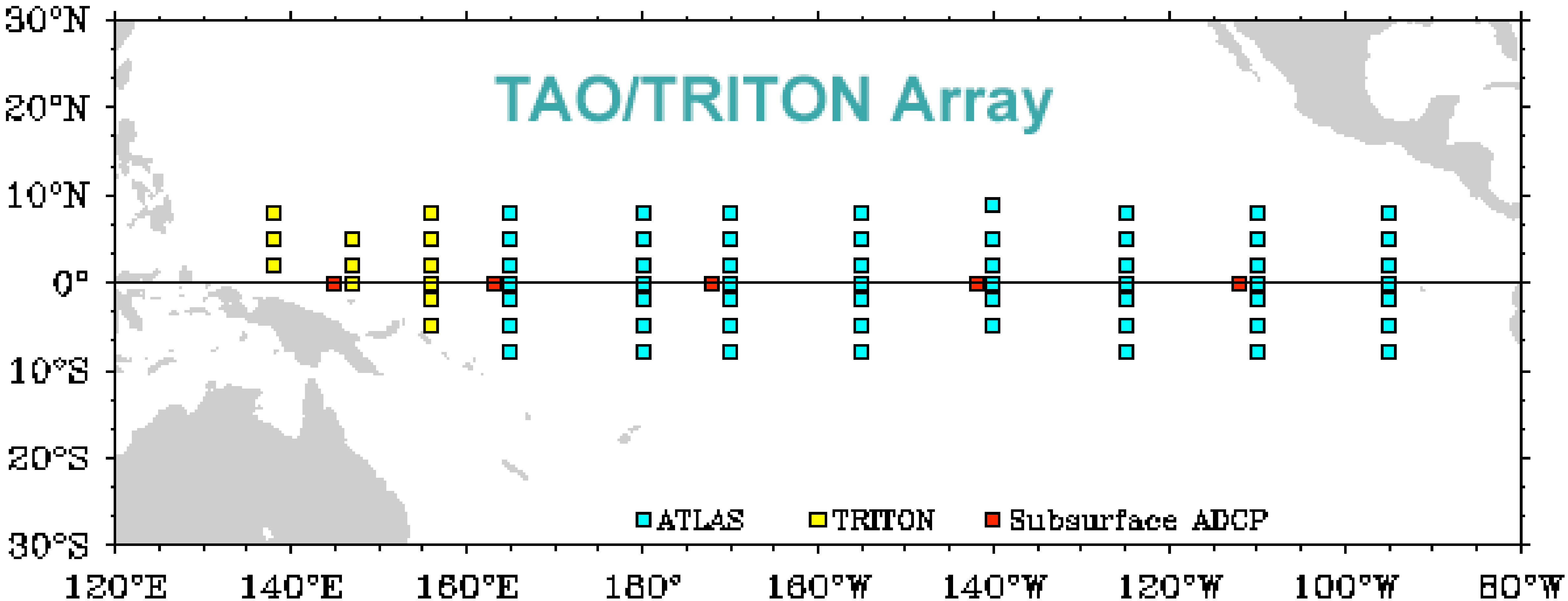

Data plots from the array are available in near-real time:

http://www.pmel.noaa.gov/tao/jsdisplay

ENSO Observing System

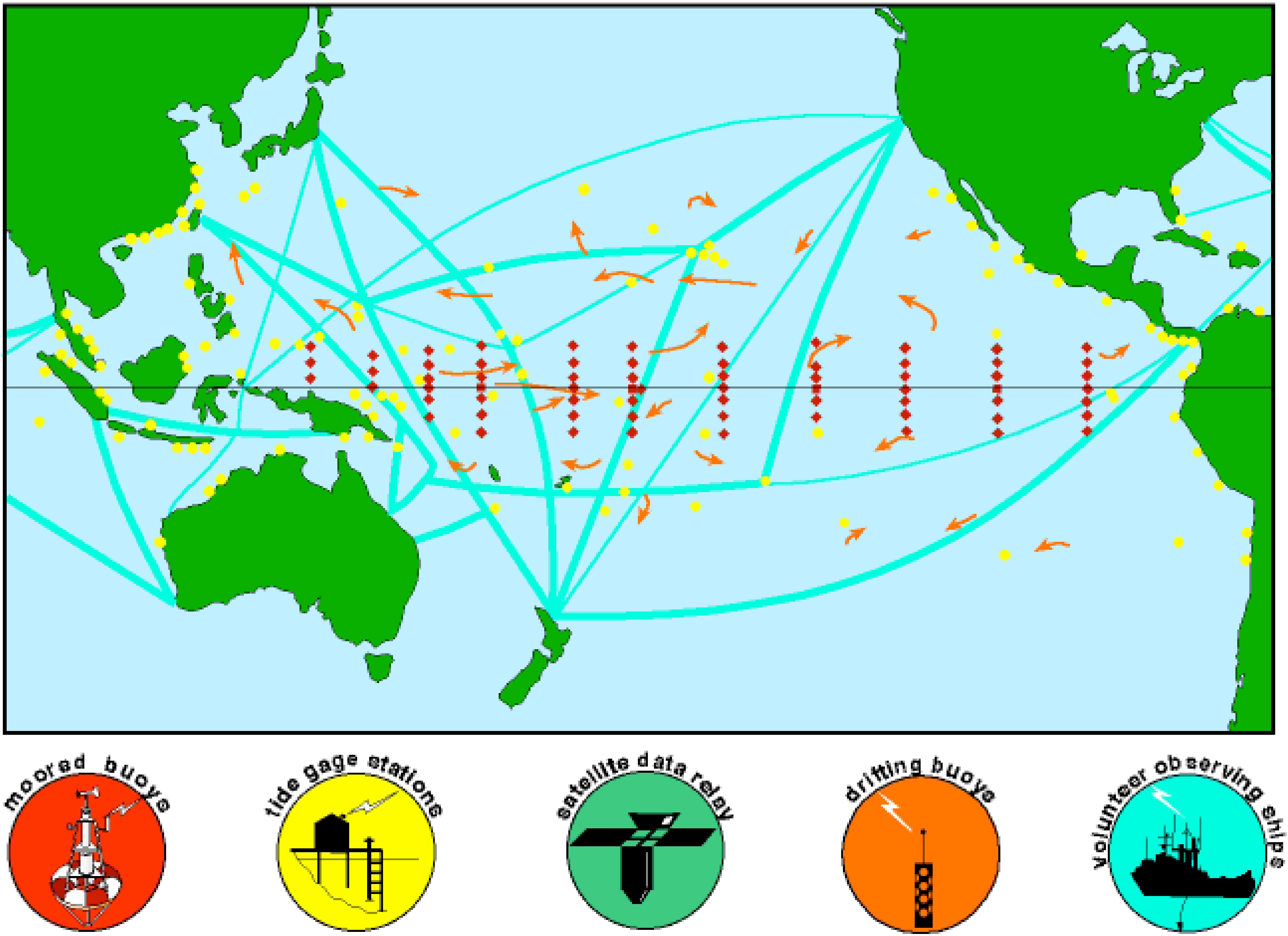

Conditions in the tropical Pacific this morning

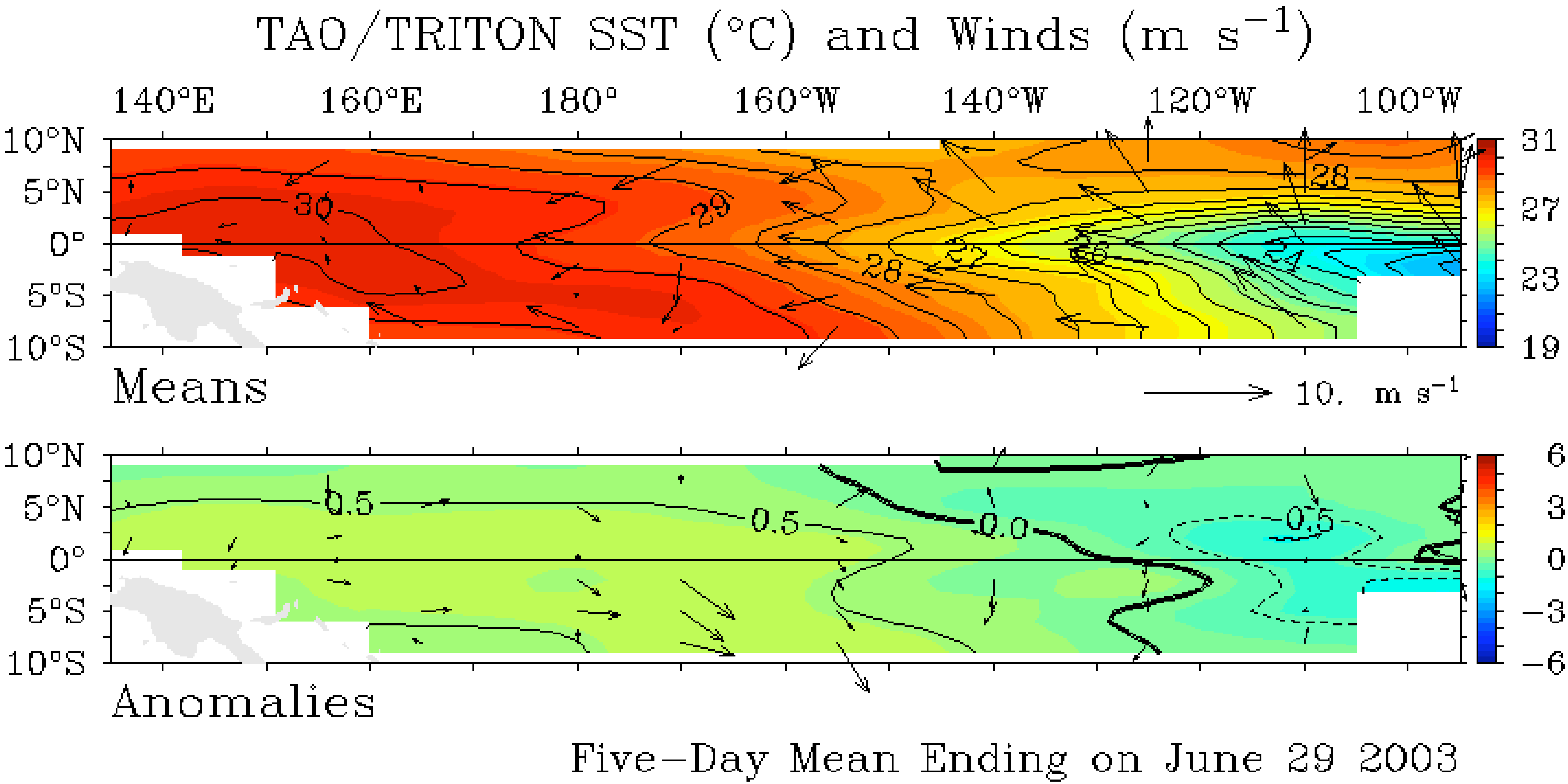

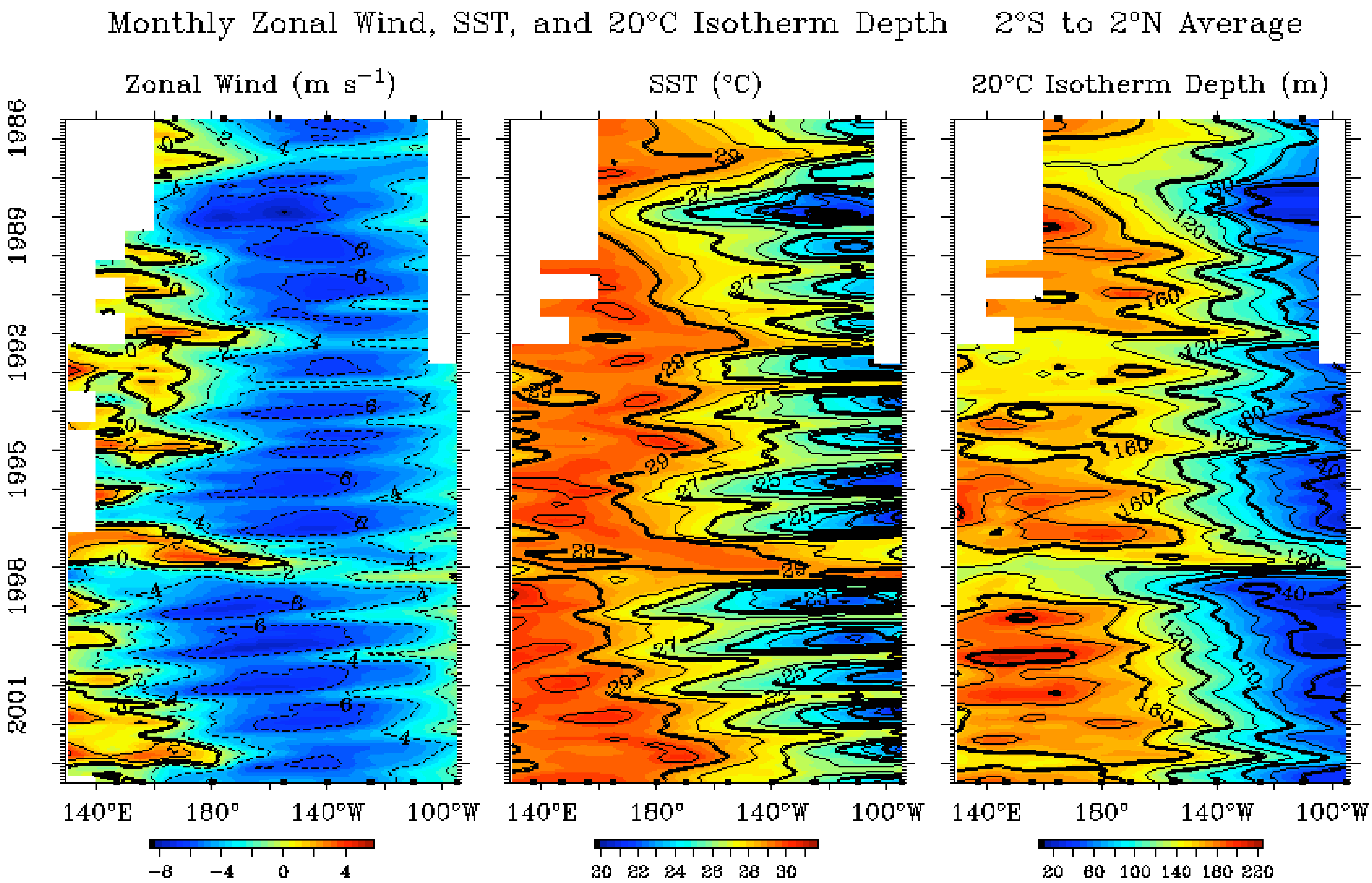

TAO Project Office/PMEL/NOAA

Jun 26 2003

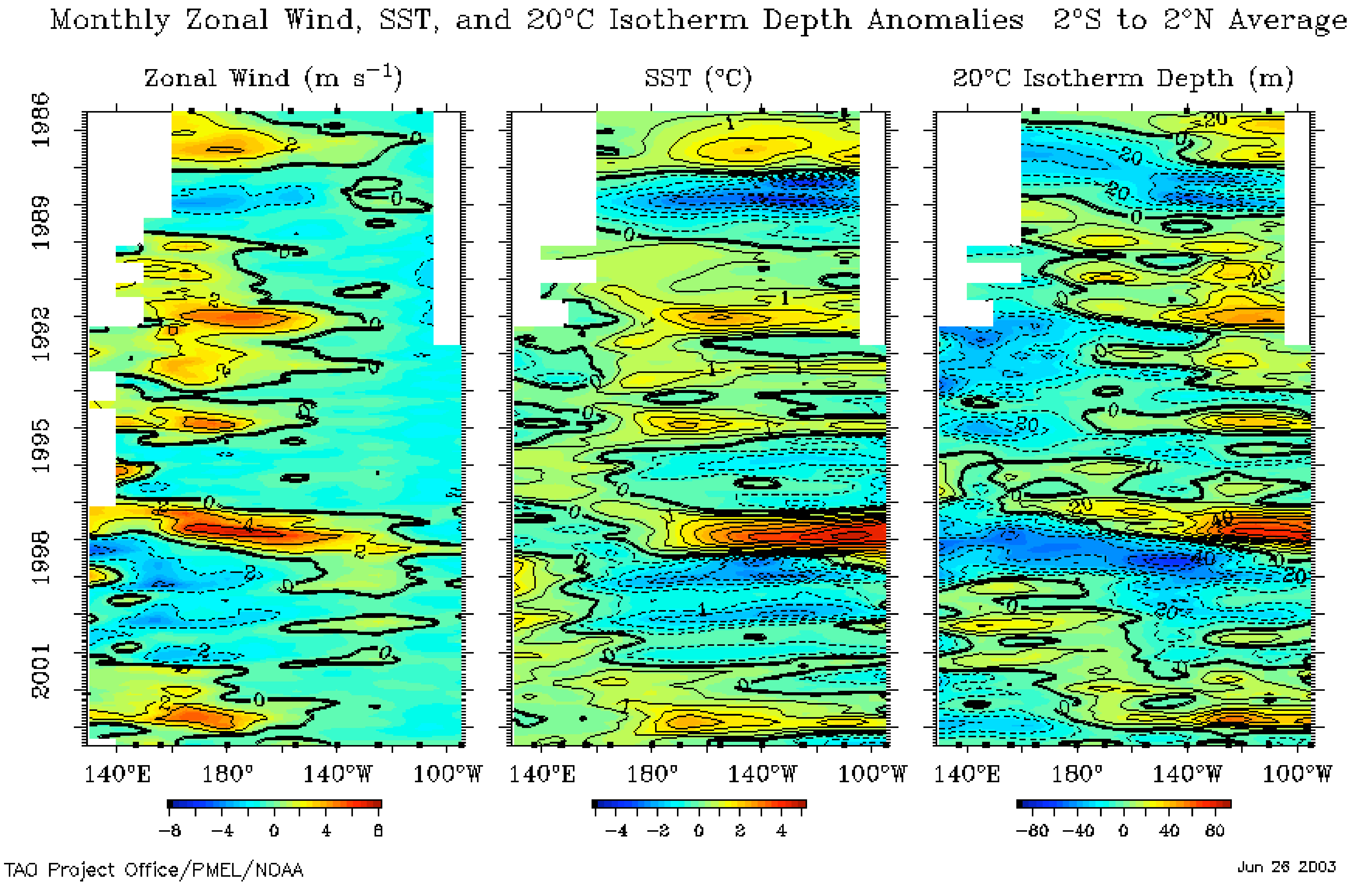

Monthly Zonal Wind, SST, and 20°C Isotherm Depth Anomalies 2°S to 2°N Average
Zonal Wind (m s⁻¹)
SST (°C)
20°C Isotherm Depth (m)
1986
1989
1992
1995
1998
2001
140°E
180°
140°W
100°W
−8
−4
0
4
8
−4
−2
0
2
4
−80
−40
0
40
80
TAO Project Office/PMEL/NOAA
Jun 26 2003

Conclusion

- The ocean-atmosphere system is *coupled*.
- We don't yet know what initiates an El Niño.
- Once an event begins, we have a good idea of how it evolves. The key to a useful forecast is recognizing the onset early.
- We have developed an array of instruments that provides early warning.

Presentation available in pdf: http://www.pmel.noaa.gov/~kessler ➙ Latest talk